QUANTITATIVE PLEISTOCENE CALCAREOUS NANNOFOSSIL BIOSTRATIGRAPHY OF LEG 86, SITE 577 (SHATSKY RISE, NW PACIFIC OCEAN)

Maria Marino, Patrizia Maiorano* & Simonetta Monechi†*

**Dipt. di Geologia e Geofisica, Univ. di Bari, Via E. Orabona, 4, 70125 Bari, Italy; marino@geo.uniba.it; †Dipt. di Scienze della Terra, Univ. di Firenze, Via La Pira, 4, 50121 Firenze, Italy*

Key words: Pleistocene, nannofossils, biochronology, Pacific Ocean, DSDP Site 577

Abstract: A quantitative study, based on calcareous nannofossil assemblages, has been carried out on the Pleistocene sediments recovered during DSDP Leg 86, from Site 577. Site 577 is located on the SW flank of the Shatsky Rise in the NW Pacific Ocean, in 2685m water-depth, and exhibits both good recovery and well-preserved nannofossil assemblages. Most conventional Pleistocene events have been recognised; moreover, quantitative investigations allowed the collection of further data on the stratigraphic distribution of some species (*Gephyrocapsa omega* >4μm, *Helicosphaera inversa*, *Reticulofenestra asanoi*, *Helicosphaera acuta*), thus improving the Pleistocene biostratigraphy of the Shatsky Rise sediments. The available magnetostratigraphic data for Site 577 also allowed the proposal of age-assignments for the following events: the last occurrence of *H. acuta*, the beginning and end of the temporary disappearance of *G. omega*, the first occurrence, temporary disappearance, and last occurrence of *H. inversa*, and the first and last occurrences of *R. asanoi*.

1. Introduction

Pleistocene nannofossil biostratigraphy has been greatly improved in recent years (Takayama & Sato, 1987; Matsuoka & Okada, 1989; Rio *et al.*, 1990; Sato *et al.*, 1991; Castradori, 1993; Raffi *et al.*, 1993; Young, 1998; Hine & Weaver, 1998; de Kaenel *et al.*, 1999; Raffi, 2002), providing further details of the definition of events and biochronology, as well as world-wide correlation. Shatsky Rise, in the NW Pacific Ocean (Figure 1), has been drilled during several DSDP and ODP legs (Legs 6, 32, 86, 132, 198) because of its proximity to the western edge of the subtropical gyre and the relatively shallow water-depth (<3000m), which has allowed good preservation of the calcareous nannofossil assemblages. However, a biostratigraphic study of Site 810 (Premoli Silva *et al.*, 1993) provided evidence of several problems with resedimentation and the presence of two hiatuses in the Pleistocene record, although no hiatuses were recognised during Leg 198 (Bralower *et al.*, 2002).

Good recovery seems to characterise the apparently continuous Pleistocene sequence at Site 577, and the high percentages of well-preserved nannofossils along with the magnetostratigraphy of Bleil (1985) make it suitable for a detailed biostratigraphic study. Previous work on the Pleistocene nannofossil assemblages of Site 577 have indicated the applicability of the standard biozonation of Okada & Bukry (1980) (Monechi, 1985), as well as of the Mediterranean scheme of Rio *et al.* (1990), and the

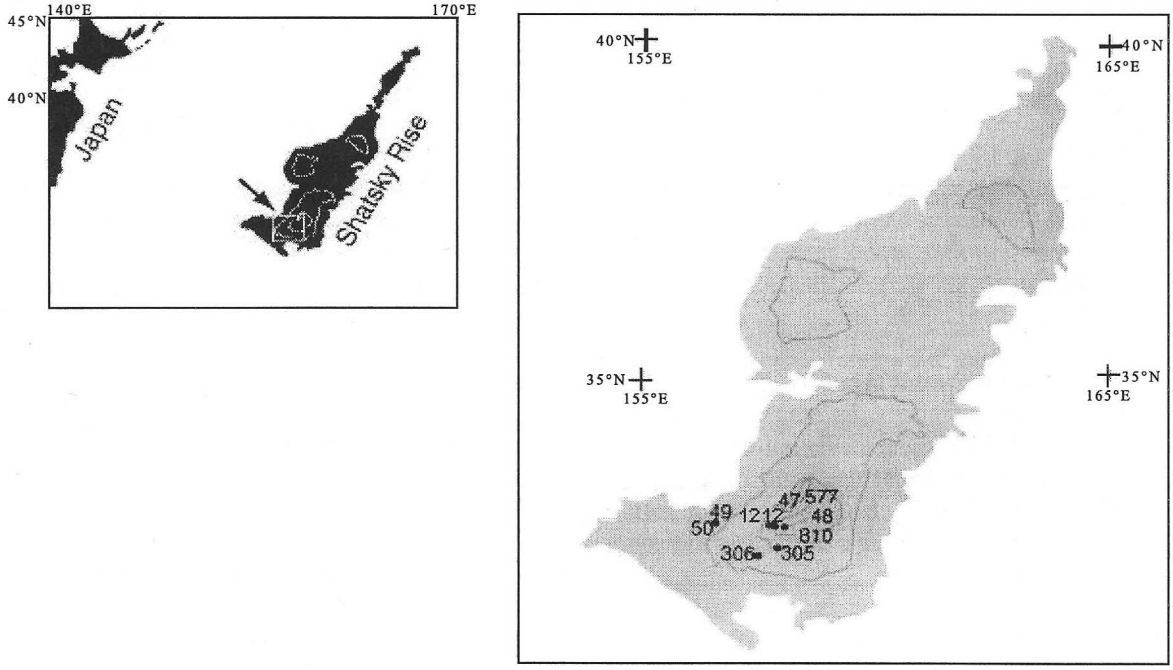

Figure 1: Location map of DSDP Site 577, and other DSDP and ODP sites on Shatsky Rise. Modified after Sliter & Brown (1993)

biozonation of Sato *et al.* (1991) for the Arabian Sea (Maiorano *et al.*, 1994), thus showing the importance of the site in global stratigraphic correlation. In particular, at Site 577, Maiorano *et al.* (1994) detected the distribution of some species (*Helicosphaera inversa, Reticulofenestra. asanoi, Gephyrocapsa omega*) whose stratigraphic significance might be enhanced by using quantitative analyses. For this purpose, we applied quantitative analysis to these assemblages.

2. Material and methods

Calcareous nannofossil assemblages from Cores 1-3 of Site 577 have been investigated in this study by means of quantitative analysis. The sediments, recovered by hydraulic-piston corer, are composed of 60-95% calcareous nannofossils, with subordinate amounts of foraminifers (0-20%), radiolarians (0-7%), and diatoms (0-3%) (Heath *et al.*, 1985). With the exception of samples 577-1-1, 140cm and 577-1- 3, 70cm, in which terrigenous concentration can occur up to 35%, the terrigenous material accounts for <15% of the sediment. Three ash-layers have been found, in samples 577-2-5, 60cm, 577-2-6, 103cm, and 577-3-1, 39cm. A few drilling disturbances are present in the hole; the recovery is 100%, 93% and 86% in Cores 1, 2, and 3, respectively (Heath *et al.*, 1985).

Smear-slides were prepared from raw sediment and examined with a light-microscope at 1000x magnification; 1600x magnification was used for the identification of very small placoliths (*e.g. Emiliania huxleyi*). Two to seven samples were investigated per section. The variable sample spacing provides a temporal resolution of 20-26kyr, down to 7kyr around some nannofossil events. Quantitative analyses were carried out on 56 samples, from the last occurrence (LO) of *Discoaster brouweri* to the increase in *E. huxleyi*. The counts were restricted to about 500 specimens of the total assemblage. This count gives a probability greater than 99% that a taxon will be encountered if its abundance in the assemblage is >1% (Crow *et al.*, 1960). Several researchers have previously used counts of 500 specimens to define selected events (*e.g.* the LO of *Pseudoemiliania lacunosa* in the Pleistocene: Thierstein *et al.*, 1977; Rio *et al.*, 1990; Castradori, 1993; Sprovieri *et al.*, 1998). In addition, counts of 50 helicoliths and 100 *Calcidiscus* spp. were carried out in order to determine abundance patterns of *Helicosphaera sellii, Helicosphaera acuta, Helicosphaera inversa,* and the LO of *Calcidiscus macintyrei*, respectively. Finally, 100 additional fields of view were scanned in order to record very rare species.

3. Taxonomic remarks

Different taxonomic criteria exist among nannofossil specialists in the identification of some Pleistocene species. Taxonomic discrepancies cause apparent differences in stratigraphical distribution and effectively compromise the biochronology. Taxonomic concepts adopted for this study are presented below.

Genus *Gephyrocapsa* Kamptner, 1943

Remarks: *Gephyrocapsa* spp. have been used to subdivide the Pleistocene due to the high abundance and rapid morphological evolution of this genus. The taxonomy of gephyrocapsids has been extensively discussed in several papers (Gartner, 1977; Raffi & Rio, 1979; Samtleben, 1980; Rio, 1982; Pujos, 1985; Rio *et al.*, 1990; Raffi *et al.*, 1993; Bollmann, 1997). The size-based subdivision of *Gephyrocapsa* summarised in Raffi *et al.* (1993) has been followed in this study because the taxonomic concepts they defined allow the recognition of large, medium, and small *Gephyrocapsa*s, which provide a high biostratigraphic resolution for this interval.

Medium *Gephyrocapsa*s are 4-5.5μm long and include specimens referable to *Gephyrocapsa caribbeanica, Gephyrocapsa oceanica* s.l. and *Gephyrocapsa omega. G. oceanica* s.l. (Plate 1, Figures 15-16) is 4-5.5μm long with an open central-area. *G. caribbeanica* (Plate 1, Figures 13-14) is 4-5.5μm long with a closed central-area. *G. omega* (Plate 1, Figures 11-12) is >4μm long with an open central-area and a bridge almost aligned with the short axis of the ellipse. *Gephyrocapsa* sp.3 *sensu* Rio (1982) and *Gephyrocapsa parallela* Hay & Beaudry, 1973 are >4μm and are herein referred to *G. omega* Bukry, 1973 >4μm. It is worth noting that the original descriptions of *G. parallela* and *G. omega* do not mention biometric criteria.

Small *Gephyrocapsa*s are <4μm in length. Large *Gephyrocapsa*s are ≥5.5μm in length.

Genus *Reticulofenestra* Hay, Molher & Wade, 1966
Reticulofenestra asanoi Sato & Takayama, 1992

Plate 1, Figures 1-2

Remarks: This species is characterised by possession of a circular to subcircular outline and is >6μm long. It corresponds to *Reticulofenestra* sp.B of Takayama & Sato (1987), and partially to the ‚small variety' (5-6.5μm long) and ‚large variety' (>6.5μm long) of circular *Reticulofenestra* sp.A of Matsuoka & Okada (1989). Different stratigraphical distributions are recorded in the literature, probably due to slightly ambiguous, different taxonomic concepts used by different authors, as discussed in Marino (1996) and Maiorano *et al.* (submitted).

Genus *Helicosphaera* Kamptner, 1954

At Site 577, *Helicosphaera* is represented by *H. carteri carteri, H. carteri hyalina, H. carteri wallichii, H. sellii, H. colombiana, H. neogranulata, H. pavimentum, H. acuta* and *H. inversa*. Among these species, *H. carteri carteri* and *H. carteri hyalina* represent the major component (Figure 2). The most stratigraphically significant abundance patterns are those of *H. sellii, H. acuta,* and *H. inversa.*

Helicosphaera inversa (Gartner, 1977) Theodoridis, 1984

Plate 2, Figures 5-16

Remarks: This species, easily recognisable at Site 577 using the original description of Gartner (1977), is characterised by a subrectangular outline, two large and rounded central-openings, an inversely-oriented bar which points toward the wing, or which is aligned with the short

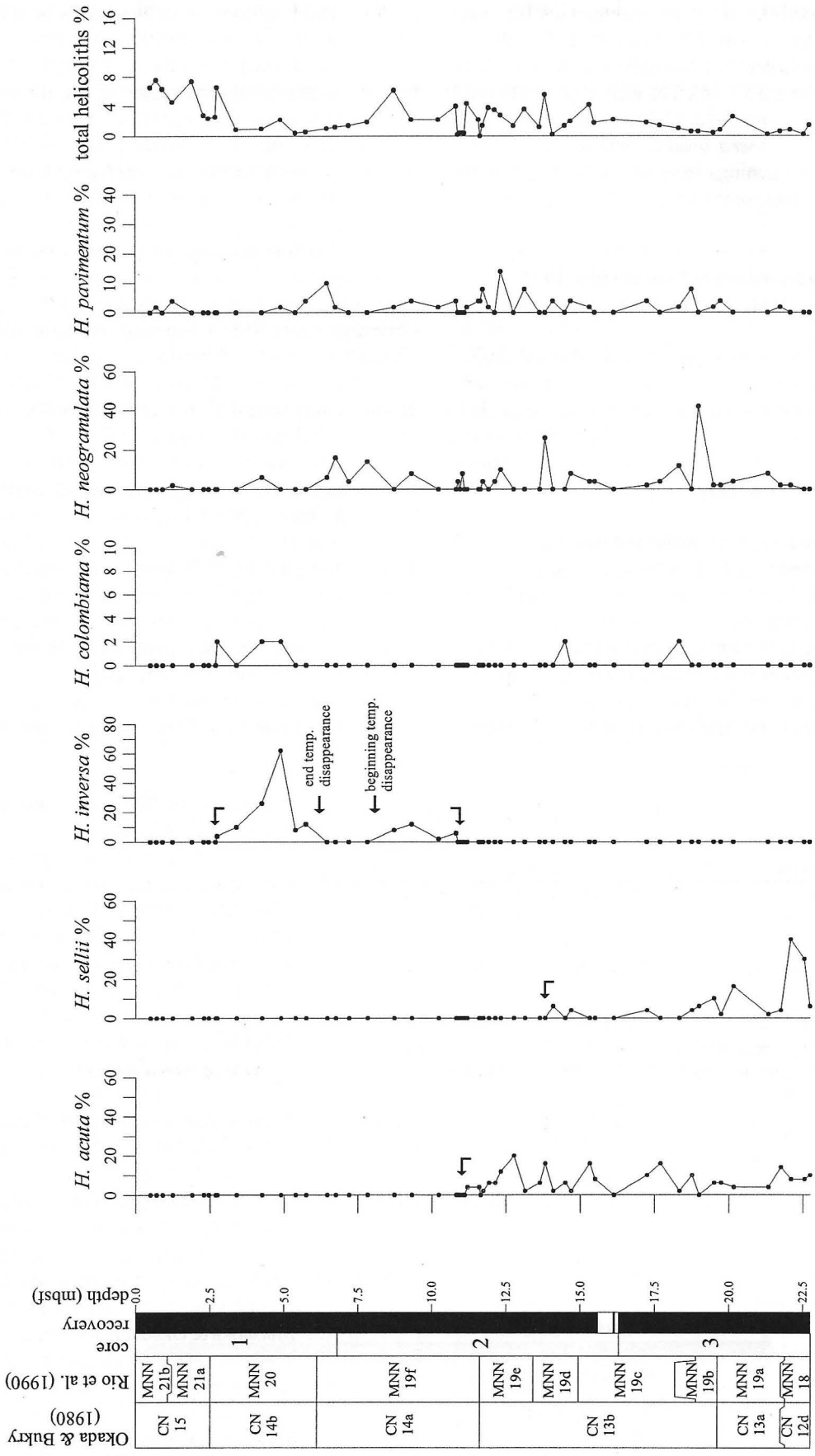

Figure 2: Abundance patterns of selected helicoliths at Site 577, based on counts of 50 helicoliths

axis of the helicolith. There is a degree of variability in the construction of the bar, and both in the width of the wing and of the central-openings of this species. In some specimens, as also indicated by Gartner (1977), the bar appears to be constructed of two halves which join at the centre (Plate 2, Figures 13-14). The wing is generally quite extended (Plate 2, Figures 5-10, 13-16), however, specimens referred to *Helicosphaera inversa* with a less-extended wing and smaller openings have also been noted at the beginning of the range of the species (Plate 2, Figures 11-12).

***Helicosphaera acuta* Theodoridis, 1984**
Plate 2, Figures 1-2

Remarks: Helicolith with a symmetrical, elliptical outline, an abrupt termination of the pointed wing, and two small, and slightly inversed, elongated central-openings. It is distinguished from other Pleistocene helicoliths by the elliptical and symmetrical outline, the smaller openings, and the abrupt, pointed wing.

4. Biostratigraphic results and discussion

Calcareous nannofossil assemblages are generally abundant and well-preserved at Site 577, with only very rare, reworked Cretaceous to Pliocene specimens in some samples. Nineteen biostratigraphic events have been recognised in the studied sediments (Table 1). Quantitative abundance patterns are shown in Figures 2 and 3. These data have allowed the application of the Pleistocene biozones of Okada & Bukry (1980) and Rio *et al.* (1990) (Figure 4).

The positions of datum-levels at Site 577, as determined here, are slightly different to those reported by Monechi (1985) and Maiorano *et al.* (1994), as a result of both the higher resolution sampling and the quantitative nature of the analyses adopted in this study. The events recognised are briefly discussed below, mainly focusing on the distributions of *Helicosphaera acuta*, *Helicosphaera inversa*, *Reticulofenestra asanoi* and *Gephyrocapsa omega*.

The LO of *Discoaster brouweri* is an event considered as globally synchronous (Backman & Shackleton, 1983; Raffi *et al.*, 1993; Wei, 1993; Chapman & Chepstow-Lusty, 1997). It defines the base of CN13a of Okada & Bukry (1980) and the base of MNN19a of Rio *et al.* (1990) (Figures 3, 4). Here, at Site 577, the LO of *D. brouweri* was recorded just 1cm below the base of the Olduvai Subchron (Figure 4), at 21.93mbsf.

The first occurrence (FO) of medium *Gephyrocapsa* (*G. oceanica* s.l. and *G. caribbeanica*) defines the base of MNN19b, correlatable to the base of CN13b. The FO of medium *Gephyrocapsa* is an easily detectable event at Site 577 (Figure 4), 49cm above the top of the Olduvai. The LO of *Calcidiscus macintyrei* at Site 577 is a distinct biostratigraphic event defining the base of MNN19c, within the lower part of CN13b (Figures 3, 4). The respective FO and LO of large *Gephyrocapsa* represent the bases of MNN19d and MNN19e of Rio *et al.* (1990) (Figure 4). At Site 577, these events are very useful for improving the Pleistocene biostratigraphy within the CN13b interval.

Events	Samples	Depth (mbsf)
E.huxleyi increase	1-1, 70-71/1-1, 90-91	0.8
E.huxleyi FO	1-2, 95-96/1-2, 119-121	2.58
H. inversa LO	1-2, 119-121/1-2, 125-126	2.725
G. omega end temp. disapp.	1-3, 40-41/1-3, 125-126	3.875
P. lacunosa LO	1-4, 90-91/1-4, 125-126	6.105
H. inversa end temp. disapp.	1-4, 125-126/1-5, 46-47	6.105
G. omega beginning temp. disapp.	1-CC, 10-11/2-1, 40-41	6.975
H. inversa beginning temp. disapp.	2-1, 103-104/ 2-2, 43-44	8.28
Brunhes-Matuyama*	2-3, 20/2-2, 130	9.8
H.inversa FO	2-3, 103-104/2-3,110-111	10.865
R.asanoi LO	2-3, 103-104/2-3,110-111	10.865
top Jaramillo*	2-3, 140/2-3, 119	11.10
G. omega FO	2-3, 131-132/2-3,139-140	11.155
H.acuta LO	2-3, 131-132/2-3,139-140	11.155
R.asanoi (>6mm) FO	2-4, 43-44/2-4, 63-64	11.83
bottom Jaramillo*	2-4, 80/2-4, 30	11.85
large *Gephyrocapsa* LO	2-5, 35-36/2-5, 85-86	13.4
H.sellii LO	2-5,103-104/2-6, 120-121	13.965
large *Gephyrocapsa* FO	2-6, 44-41/2-6, 103-104	15.415
C. macintyrei LO	3-2, 96-97/3-2, 119-121	18.88
medium *Gephyrocapsa* FO	3-3, 20-21/3-3, 44-45	19.62
top Olduvai*	3-4, 41/3-2, 120	0,8409722
bottom Olduvai*	3-4, 85/3-4, 140	21.92
D. brouweri LO	3-4, 96-97/3-4, 130-131	21.93

Table 1: Calcareous nannofossil events at Site 577. FO = first occurrence; LO = last occurrence. *Magnetic data from Bleil (1985)

The LO of *Helicosphaera sellii* is considered diachronous (Backman & Shackleton, 1983; Raffi *et al.*, 1993; Wei, 1993). It is not easily detectable at Site 577; the abundance pattern of the species indicates that it is discontinuously present in its final range, and a very low abundance of helicoliths is recorded from the lower part of the studied section (Figure 2). However, we tentatively place the LO of *H. sellii* in the uppermost part of MNN19d, slightly below the LO of large *Gephyrocapsa* (Table 1, Figures 2, 4), at 13.965mbsf.

Despite taxonomic discrepancies concerning *Reticulofenestra asanoi*, the FO and LO of the species (see taxonomic remarks, above) are considered useful events in the Pleistocene (Takayama & Sato, 1987; Matsuoka & Okada, 1989; Sato & Takayama, 1992; Wei, 1993; Raffi, 2002). Many authors refer to the 'bottom acme', or last common occurrence (Sato *et al.*, 1991; Marino, 1996; Maiorano *et al.*, submitted), and 'top acme' (Takayama & Sato, 1987; Sato *et al.*, 1991; Spaulding, 1991; Marino, 1996; Maiorano *et al.*, submitted) of *R. asanoi*, the abundance pattern of which shows the

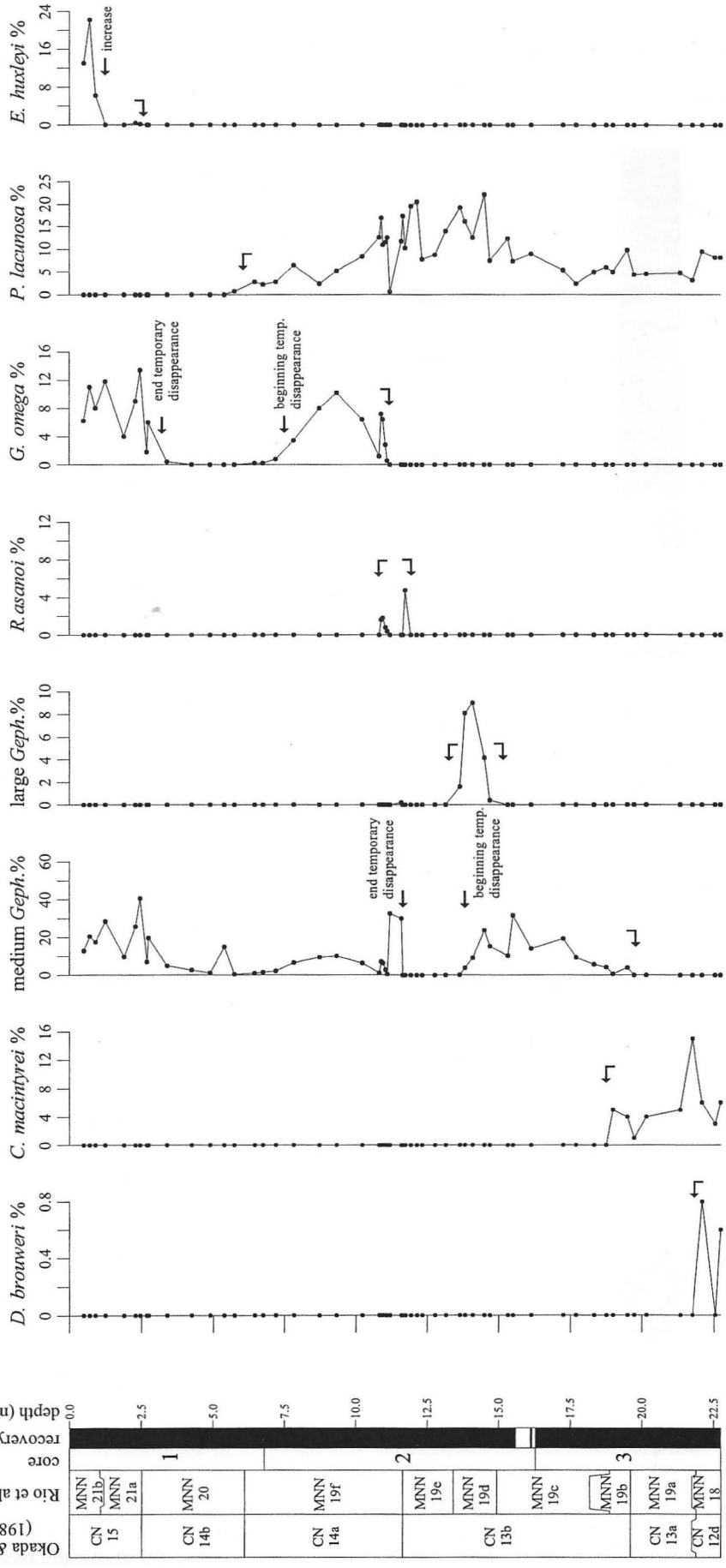

Figure 3: Abundance patterns of selected calcareous nannofossils at Site 577, determined by counting 500 specimens. Percentage of *Calcidiscus macintyrei* is based on counts of 100 specimens of *Calcidiscus*

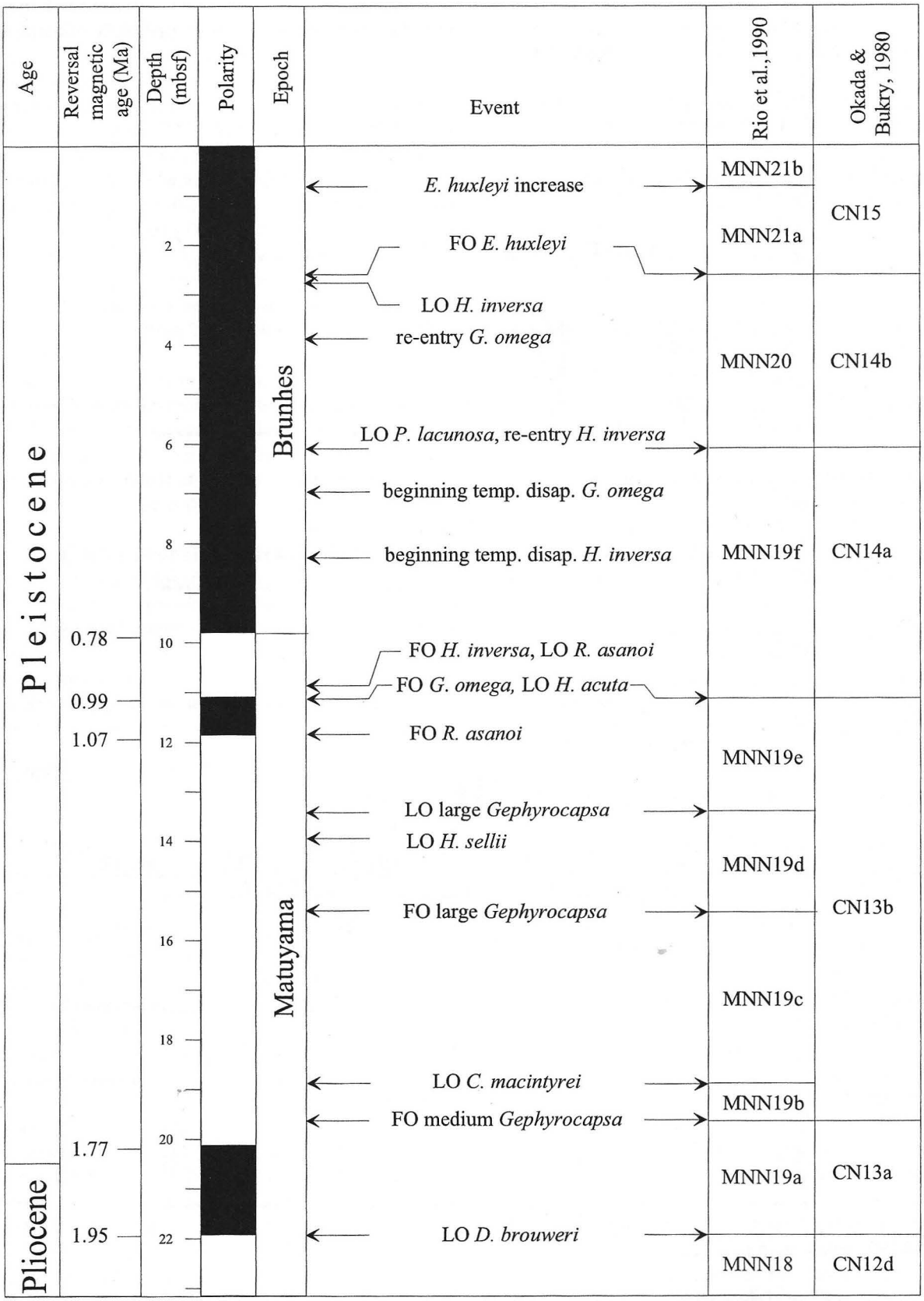

Figure 4: Nannofossil biostratigraphic events and biozonation at Site 577. Magnetostratigraphy after Bleil (1985); magnetic boundary ages from Shackleton *et al.* (1990)

presence of very few specimens at the beginning and end of its stratigraphical distribution. At Site 577, *R. asanoi* has a very short-lived distribution, from the upper part of MNN19e to the lower part of MNN19f. In particular, the species ranges from just above the base of the Jaramillo Subchron to just above the top of the Jaramillo. Whereas the FO is considered to be diachronous, the disappearance of the species is mainly reported as occurring close to

Oxygen Isotope Stage (OIS) 22 or to the transition 22/23 (Wei, 1993; Raffi, 2002; Maiorano *et al.*, submitted).

The re-entry of medium *Gephyrocapsa*, generally associated with the FO of *Gephyrocapsa omega*, marks the MNN19e/MNN19f boundary according to Rio *et al.* (1990) (Figures 3, 4). The event is not considered to be synchronous on a global scale because it has been correlated to different isotope stages, from 29 to 25 (Raffi *et al.*, 1993; Wei, 1993; Castradori, 1993; Sprovieri *et al.*, 1998; Raffi, 2002; Maiorano *et al.*, submitted). The diachroneity of this event seems to involve migration from equatorial to high latitudes (Wei, 1993; Raffi 2002), and also a different sample resolution. At Site 577, the re-entry of medium *Gephyrocapsa* occurs at 11.625mbsf, approximately 50cm below, not together with, the FO of *G. omega*, that represents the main component of medium *Gephyrocapsa* from its FO at 11.15mbsf to approximately 8mbsf.

The LO of *Helicosphaera acuta* has not been reported in the literature, and only few biostratigraphic data are available on the distribution of this species. According to Theodoridis (1984), *H. acuta* ranges from CN12 to CN13 (Middle-Late Pliocene to Pleistocene) whilst Liu *et al.* (1996) recorded the species from the Late Pliocene. A Pleistocene abundance pattern for *H. acuta* is recorded herein: the species is well represented within the genus (4-17%: Figure 2), although it is rare as part of the total nannofossil assemblage; its LO is recorded at 11.15mbsf, within CN14a (MNN19f), slightly above the Jaramillo (Figure 4). This bioevent, not recognised by Maiorano *et al.* (1994) due to the rarity of the species, requires quantitative analysis of the genus; however, the potential biostratigraphic validity of this event must be tested elsewhere.

The FO and LO of *Helicosphaera inversa* are valuable biostratigraphic events at Site 577, however, the distribution of this species is also poorly documented in the literature. The abundance pattern of *H. inversa* at Site 577 shows rare and scattered specimens first occurring at the base of CN14a/MNN19f, just above the top of the Jaramillo (Figures 2, 4); continuous and common occurrences were then recorded within CN14b/MNN20. The FO of *H. inversa* at Site 577 does not seem to be in agreement with data from Takayama & Sato (1987), Spaulding (1991), Sato & Takayama (1992), nor Maiorano *et al.* (1994), all of whom place the FO of *H. inversa* at a younger level; Hine (1990) correlated the FO of *H. inversa* to OIS 12-13, supporting a younger age for this event. Discrepancies may be due to the methods adopted by different authors for the recognition of the FO and LO of helicoliths (*i.e.* counting related to total assemblages, or to helicoliths alone), or to the ecological preferences of the species (Takayama & Sato, 1987). It is noteworthy that an interval of temporary disappearance of *H. inversa* in the middle part of its distribution, within upper CN14a, corresponds to a low abundance of total helicoliths in the nannofossil assemblages. The LO of *H. inversa* at Site 577 falls just below the FO of *Emiliania huxleyi*, at the top of CN14b/MNN20, whilst in the North Atlantic Ocean this event is recorded above the FO of *E. huxleyi* (Takayama & Sato, 1987; Sato & Takayama, 1992). The diachronous character of the LO of *H. inversa* is also confirmed by Hine (1990), who indicated a time-transgressive occurrence of >47kyr.

The abundance pattern of *Gephyrocapsa omega* (Figure 3) shows a distinct temporary disappearance, ranging from the upper part of MNN19f to middle MNN20. A paracme interval of *G. omega* within the Pleistocene has been noted within MNN19f in the Mediterranean area by various authors (Castradori, 1993; Marino, 1996; Maiorano *et al.*, submitted), where this morphotype last occurs at 0.584Ma (Castradori, 1993), very close to OIS 15 (Sprovieri *et al.*, 1998). However, Matsuoka & Okada (1989) recorded a temporary disappearance of *Gephyrocapsa parallela* (= *G. omega*) in the NW Pacific Ocean at a stratigraphic level comparable to that recorded at Site 577, according to Maiorano *et al.* (1994). The distribution of *G. omega* could be ecologically controlled, however, investigation of different localities might clarify the biostratigraphic utility of the paracme event on a regional scale, and shed light on the palaeoecological controls on its distribution.

The LO of *Pseudoemiliania lacunosa*, considered a globally synchronous event in OIS 12, is easily detectable at Site 577, allowing the recognition of the base of CN14b/MNN20 (Figures 3, 4). The FO of *Emiliania huxleyi* marks the base of CN15/MNN21a and is also considered to be globally synchronous, correlatable to OIS 8 according to the majority of published sources (Thierstein *et al.*, 1977; Rio *et al.*, 1990; Berggren *et al.*, 1995; Sprovieri *et al.*, 1998), although some authors have correlated the FO of *E. huxleyi* to OIS 7 (Sigl & Muller, 1975; Blechschmidt *et al.*, 1982; Erba *et al.*, 1987). At Site 577, the base of CN15/MNN21a has been recognised on the basis of the first rare occurrence of *E. huxleyi* (Figures 3, 4) observed with the light-microscope. The increase in abundance of *E. huxleyi*, proposed by Gartner (1977) to define the base of the *E. huxleyi* Acme Zone, seems to be a distinctive event at Site 577; it allowed the base of MNN21b to be recognised (within CN15).

The presence of all zonal events suggests a continuous Pleistocene sedimentary record at Site 577. The co-occurrence of some additional events (LO *H. acuta* together with FO *G. omega*; LO *R. asanoi* with FO *H. inversa*; beginning of temporary disappearance of *G. omega* with LO *P. lacunosa*: Figure 4) might, however, indicate condensed intervals or slight sedimentary disturbances. No extensive hiatuses were detected, as recorded by Premoli Silva *et al.* (1993) at Hole 810C, (SW Shatsky Rise), where the small *Gephyrocapsa* and the *Calcidiscus macintyrei* Zones of Gartner (1977) are missing.

5. Magnetobiochronology

The quantitative calcareous nannofossil analyses performed in this study, plotted against the magnetostratigraphic data of Bleil (1985), have allowed the assignment of ages for some of these events (Table 2), from the Jaramillo Subchron to the increase in *Emiliania huxleyi*. The ages were obtained using the astronomical calibration of the magnetic boundaries according to Shackleton *et al.* (1990). In addition, the *E. huxleyi* abundance increase at 0.09Ma and the LO of *Pseudoemiliania lacunosa* at 0.46Ma (according to

Nannofossil events	This work	Takayama & Sato (1987)	Matzuoka & Okada (1989)	Sato & Takayama (1992)	Wei (1993)	Berger *et al.* (1994)	de Kaenel *et al.* (1999)	Raffi (2002)
LO *H. inversa*	0.224	0.15	0.54	0.15				
G. omega end temp. disapp.	0.304		0.3					
H. inversa end temp. disapp.	0.46							
G. omega beginning temp. disapp.	0.53		0.5					
H. inversa beginning temp. disapp.	0.649							
FO *H. inversa*	0.818	0.48	0.8	0.48				
LO *R. asanoi*	0.818		0.81 (>6.5mm)	0.83	0.88-0.92*	0.889	0.781-0.785*	0.89-0.91*
LO *H. acuta*	0.995							
FO *R. asanoi*	1.06		0.98 (>6.5mm)	1.06	1.02-1.17*	1.168	1.122*	1.11-1.18*

Table 2: Nannofossil event ages from this work compared to biochronology from published sources. Asterisks indicate slight differences in taxonomic concept between authors

Berggren *et al.*, 1995), were considered as calibration points. A comparison between previously-published age-assignments for Pleistocene datum-levels and those obtained during this study is also presented in Table 2. A sedimentation rate curve for Site 577 has been drawn, using the ages of the five calibration points mentioned above (Figure 5).

The FO of *Reticulofenestra asanoi* at Site 577 is correlatable with the data of Sato & Takayama (1992), who formally described the species, restricting the species to circular-subcircular forms >6μm, as considered in this study. The LO of *R. asanoi*, at 10.865mbsf, has an age of 0.818Ma, correlatable with the age-assignments of Matsuoka & Okada (1989) and Sato & Takayama (1992). Differences in taxonomic concept, or in the age-calibration methodology, as well as in sample resolution may have caused the biochronological discrepancies between the work herein and the determinations of other authors (Table 2); in particular, significant diachroneity (up to 140kyr) is noted for the age of the LO of *R. asanoi,* compared to the data of de Kaenel *et al.* (1999), who reported large forms (up to 12μm long) in OIS 19, thus providing the youngest age-assignment in the literature.

The LO of *Helicosphaera acuta* is estimated to be at 0.995Ma. This event is coincident with the FO of *Gephyrocapsa omega*, at 11.155mbsf, just below the top of the Jaramillo. In this interval, sedimentation rates are lower than above and below; an inconsistent deposition rate, combined with several very short hiatuses (due to contour currents or turbidity flows) has been postulated for Site 577 by Sager *et al.* (1993). Polgreen *et al.* (1993) agreed with this opinion, because the Plio-Pleistocene magnetic susceptibility cycles from Hole 810C do not match with those at Site 577, which is located only 11km to the west and is 50m deeper. This idea could also explain the coincident FO of *Helicosphaera inversa* and LO of *R. asanoi* at 10.865mbsf (Figures 5, 6). The FO of *H. inversa* at 0.818Ma is in good agreement with Matsuoka & Okada (1989), whereas significantly younger dates were proposed by Takayama & Sato (1987) and Sato & Takayama (1992). At Site 577, the pattern of *H. inversa* shows a temporary disappearance before the extinction; the ages proposed for the beginning and end of this temporary disappearance at Site 577 are 0.649Ma and 0.46Ma, respectively. Note that the age of the end of this temporary disappearance (0.46Ma) is very close to that proposed for the FO of the species (0.48Ma) by Takayama & Sato (1987) and Sato & Takayama (1992); this may suggest that the rarity of the taxon in its lower distribution make it difficult to recognise its FO. The LO of *H. inversa* is here estimated to be 0.224Ma; different age assignments are reported for this event by different authors (Table 2) and a diachroneity over 47kyr was suggested by Hine (1990). However, the quantitative abundance pattern of *H. inversa* is currently poorly known and therefore the discrepancies in the age-assignment for the FO and LO of the species cannot be clearly explained.

The dates for the beginning and end of the temporary disappearance of *Gephyrocapsa omega* have been estimated at 0.53 and 0.304Ma, respectively, at Site 577 (Table 2). These ages seem to be in relative agreement with previous calibrations made by Matsuoka & Okada (1989) from the NW Pacific Ocean, although the onset of the temporary disappearance of *G. omega* is apparently diachronous by 30kyr.

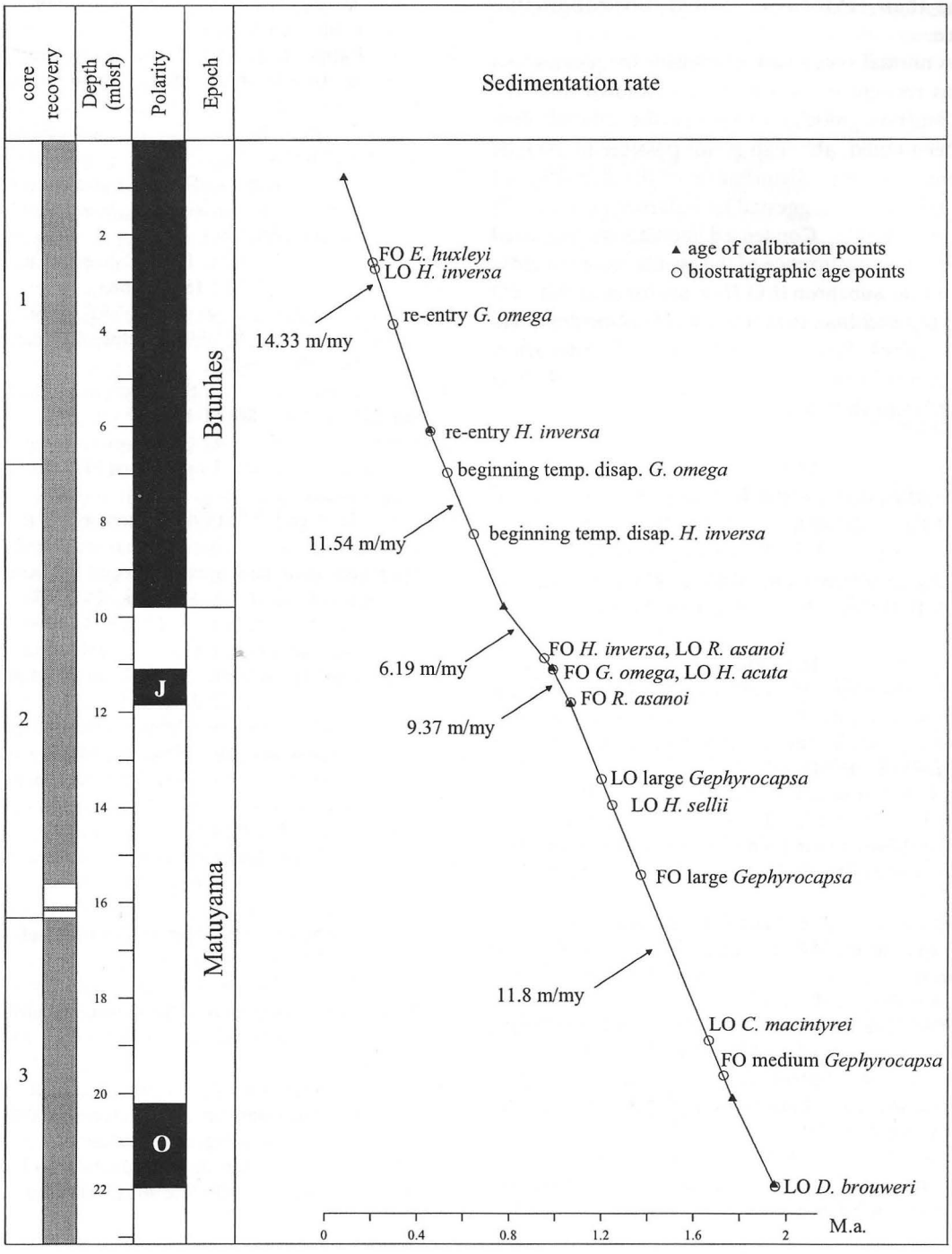

Figure 5: Sedimentation rate at Site 577

6. Concluding remarks

A quantitative study of the calcareous nannofossil assemblages at Site 577 has allowed the application of the biozonation schemes of Okada & Bukry (1980) and Rio *et al.* (1990).

The biostratigraphic events have been correlated to the magnetostratigraphy of Bleil (1985), providing biochronologic data for some events which have been under-reported in the literature, including: the LO of *Helicosphaera acuta*; temporary disappearance of *Gephyrocapsa omega*; FO, temporary disappearance, and LO of *Helicosphaera inversa*; FO and LO of *Reticulofenestra asanoi*.

Most of the dates correlate well with previous reports, however some discrepancies do appear among authors. They are possibly due to the different methods of analysis used for estimating dates, to different taxonomic concepts of species (especially *R. asanoi*), and to different sampling resolutions. The temporary disappearance of *G. omega* appears to be younger (from the upper part of CN14a to the basal part of CN14b) in the Pacific Ocean than in the Mediterranean area, where it occurs earlier, within CN14a/MNN19f (Castradori, 1993; Maiorano *et al.*, submitted).

The quantitative stratigraphical distributions of *H. inversa* and *H. acuta* have been documented and could be used to improve nannofossil biostratigraphy in the upper part of the Pleistocene. The proposed age-assignments, however, need to be tested at other locations in order to

determine their regional or global biostratigraphic importance.

A normal succession of Pleistocene nannofossil events was recognised at Site 577, as known from the literature, and no significant variation in the sedimentation rate has been noted, although is not possible to exclude the presence of some disturbance in the depositional history at this site, as suggested by Polgreen *et al.* (1993) and Sager *et al.* (1993). Condensed intervals are suggested by the coincident occurrence of the events recorded close to the Jaramillo Subchron (LO *H. acuta* together with FO *G. omega*; LO *R. asanoi* together with FO *H. inversa*) and in the Brunhes Epoch (beginning of temporary disappearance of *G. omega* together with LO *Pseudoemiliania lacunosa*).

Acknowledgements

We are grateful to H. Okada & J. Lees for their careful reviews of the manuscript. This research used samples provided by the DSDP. The study was financially supported by an MIUR Grant 40% (2001) to N. Ciaranfi, and by an MIUR Grant 40% (2001) to S. Monechi.

References

Backman, J. & Shackleton, N.J. 1983. Quantitative biochronology of Pliocene and early Pleistocene calcareous nannofossils from the Atlantic, Indian and Pacific oceans. *Mar. Micropaleontol.*, **8:** 141-170.

Berggren, W.A., Hilgen, F.J., Langereis, C.G., Kent, D.V., Obradovich, J.D., Raffi, I., Raymo, M.E. & Shackleton, N.J. 1995. Late Neogene chronology: New perspectives in high-resolution stratigraphy. *Geol. Soc. Am. Bull.*, **107:** 1272-1287.

Blechschmidt, G., Cita, M.B., Mazzei, R. & Salvatorini, G. 1982. Stratigraphy of the Western Mediterranean and Southern Calabrian ridges, eastern Mediterranean. *Mar. Micropaleontol.*, **7:** 101-134.

Bleil, U. 1985. The magnetostratigraphy of northwest Pacific sediments, DSDP Leg 86. *IRDSDP,* **86:** 441-458.

Bollmann, J. 1997. Morphology and biogeography of *Gephyrocapsa* coccoliths in Holocene sediments. *Mar. Micropaleontol.*, **29:** 319-350.

Boudreaux, J.E. & Hay, W.W. 1969. Calcareous nannoplankton and biostratigraphy of the Late Pliocene-Pleistocene-Recent sediments in the Submarex cores. *Rev. Esp. Micropaleontol.,* **1:** 249-292.

Bralower, T.J., Premoli Silva, I., Malone, M.J. *et al.*, 2002. *Proc. ODP, Init. Repts,* 198 [CD-ROM]. Ocean Drilling Program, Texas A&M University, College Station TX 77845-9547, USA.

Bukry, D. 1973. Coccolith stratigraphy, eastern equatorial Pacific, Leg 16, DSDP. *IRDSDP,* **16:** 653-711.

Bukry, D. 1979. Neogene coccolith stratigraphy, Mid Atlantic Ridge, DSDP Leg 45. *IRDSDP,* **45:** 307-317.

Bukry, D. & Bramlette, M.N. 1969. Some new and stratigraphically useful calcareous nannofossils of the Cenozoic. *Tulane Stud. Geol. Paleontol.,* **7:** 131-142.

Castradori, D. 1993. Calcareous nannofossil biostratigraphy and biochronology in eastern Mediterranean deep-sea cores. *Riv. It. Paleont. Strat.*, **99:** 107-126.

Chapman, M.R. & Chepstow-Lusty, A.J. 1997. Late Pliocene climatic change and the global extinction of the discoasters: an independent assessment using oxygen isotope records. *Palaeogeogr., Palaeoclimatol., Palaeoecol.*, **134:** 109-125.

Crow, F.L., Davis, F.G. & Maxfield, M.W. 1960. *Statistic manual.* Dover Publ., New York.

Erba, E., Parisi, E. & Cita, M.B. 1987. Stratigraphy and sedimentation in the western Strabo Trench, Eastern Mediterranean. *Mar. Geol.*, **75:** 57-75.

Gaarder, K.R. 1970. Three new taxa of Coccolithinae. *Nytt Mag. Bot.,* **17:** 113-126.

Gartner, S. 1977. Correlation of Neogene planktonic Foraminifera and Calcareous Nannofossil zones. *Trans. Gulf Coast Assoc. Geol. Soc.*, **19:** 585-599.

Hay, W.W. & Beaudry, F.M. 1973. Calcareous nannofossils – Leg 15, DSDP. *IRDSDP,* **15:** 625-683.

Hay, W.W., Mohler, H.P. & Wade, M.E. 1966. Calcareous nannofossils from Nal'chik (northwest Caucasus). *Eclog. Geol. Helv.*, **59:** 379-399.

Heath, G.R., Burckle, L.H. & Shipboard Scientific Party, 1985. Site 577. *IRDSDP,* **86:** 91-137.

Hine, N. 1990. *Late Cenozoic Calcareous Nannoplankton from the Northeast Atlantic.* Unpublished PhD thesis, University of East Anglia.

Hine, N. & Weaver, P.P.E. 1998. Quaternary. *In*: P. Bown (Ed.). *Calcareous nannofossil biostratigraphy.* British Micropaleontological Society Special Publications Series, Chapman & Hall/Kluwer Academic: 265-283.

de Kaenel, E., Siesser, W.G. & Murat, A. 1999. Pleistocene calcareous nannofossil biostratigraphy and the western Mediterranean sapropels, Sites 974 to 977 and 979. *Proc. ODP, Sci. Res.*, **161:** 159-183.

Kamptner, E. 1941. Die Coccolithineen der Südwestküste von Istrien. *Ann. Naturh. Mus. Wien,* **51:** 54-159.

Kamptner, E. 1943. Zur Revision der Coccolithineen-Spezies *Pontosphaera huxleyi* Lohmann. *Anz. Acad. Wiss. Wien, Math.-Naturw. Kl.*, **80:** 43-49.

Kamptner, E. 1954. Untersuchungen über den Feinbau der Coccolithen. *Arch. Protistenk.*, **100:** 1-90.

Liu, L., Maiorano, P. & Zhao, X. 1996. Pliocene-Pleistocene calcareous nannofossils from the Iberia plain. *Proc. ODP, Sci. Res.*, **149:** 147-164.

Lohmann, H. 1902. Die Coccolithophoridae, eine Monographie der Coccolithen bildenden Flagellaten, zugleich ein Beitrag zur Kenntnis des Mittelmeerauftriebs. *Arch. Protistenk.,* **1:** 89-165.

Maiorano, M., Marino, M., Di Stefano, E. & Ciaranfi, N. Submitted. Calcareous nannofossil events and calibration with oxygen isotope and sapropel stratigraphy in the Lower-Middle Pleistocene transition at Montalbano Jonico section (Southern Italy) and ODP Site 964 (Ionian Sea). *Quaternary Intern.*

Maiorano, M., Marino, M. & Monechi, S. 1994. Pleistocene calcareous nannofossil high resolution biostratigraphy of Site 577, Northwest Pacific Ocean. *Palaeopelagos,* **4:** 119-128.

Marino, M. 1996. Quantitative calcareous nannofossil biostratigraphy of Lower-Middle Pleistocene Montalbano Ionico section (Southern Italy). *Palaeopelagos,* **6:** 347-360.

Matsuoka, H. & Okada, H. 1989. Quantitative analysis of Quaternary nannoplankton in the Subtropical Northwestern Pacific Ocean. *Mar. Micropaleontol.*, **14:** 97-118.

Monechi, S. 1985. Campanian to Pleistocene calcareous nannofossil stratigraphy from the Northwest Pacific Ocean, Deep Sea Drilling Project Leg 86. *IRDSDP,* **86:** 301-336.

Okada, H. & Bukry, D. 1980. Supplementary modification and introduction of code numbers to the low-latitude coccolith biostratigraphic zonation (Bukry, 1973; 1975). *Mar. Micropaleontol.*, **5:** 335-353.

Okada, H. & MacIntyre, A. 1977. Modern Coccolithiphores of the Pacific and North Atlantic Oceans. *Micropalentology,* **23:** 1-55.

Norris, R.E. 1965. Living cells of *Ceratolithus cristatus* (Coccolithophorineae). *Arch. Protistenk.*, **108:** 19-24.

Polgreen, E.L., Sager, W.W., Rack, F.R. & van Waasbergen, R.J. 1993. Magnetic properties of Pliocene-Pleistocene sediments from Hole 810C, Shatsky Rise, and implication for the origin and correlability of their magnetic susceptibility variations. *Proc. ODP, Sci. Res.*, **132:** 37-45.

Premoli Silva, I., Castradori, D. & Spezzaferri, S. 1993. Calcareous nannofossil and planktonic foraminifer biostratigraphy of Hole 810C (Shatsky Rise, Northwestern Pacific). *Proc. ODP, Sci. Res.*, **132:** 15-33.

Pujos, A. 1985. Quaternary nannofossils from Goban Spur, eastern north Atlantic Ocean, Deep Sea Drilling Project Holes 548 and 549A. *IRDSDP,* 80: 767-792.

Raffi, I. 2002. Revision of the early-middle Pleistocene calcareous nannofossil biochronology (1.75-0.85 Ma). *Mar. Micropaleontol.*, **45:** 25-55.

Raffi, I., Backman, J., Rio, D. & Shackleton, N.J. 1993. Early Pleistocene and late Pliocene nannofossil biostratigraphy and calibration to oxygen isotope stratigraphies from DSDP Site 607 and ODP Site 677. *Paleoceanography*, **8:** 387-404.

Raffi, I. & Rio, D. 1979. Calcareous nannofossil biostratigraphy of DSDP Site 132-Leg 13 (Tyrrhenian Sea-Western Mediterranean). *Riv. It. Paleontol. Strat.*, **85:** 127-172.

Rio, D. 1982. The fossil distribution of Coccolithophore Genus *Gephyrocapsa* Kamptner and related Pliocene-Pleistocene chronostratigraphic problems. *IRDSDP,* **68:** 325-343.

Rio, D., Raffi, I. & Villa, G. 1990. Pliocene-Pleistocene calcareous nannofossil distribution patterns in the Western Mediterranean. *Proc. ODP, Sci. Res.*, **107:** 513-533.

Sager, W.W., Polgreen, E.L. & Rack, F.R. 1993. Magnetic polarity reversal stratigraphy of Hole 810C, Shatsky Rise, Western Pacific Ocean. *Proc. ODP, Sci. Res.*, **132:** 47-55.

Samtleben, C. 1980. Die Evolution der Coccolithophoriden-Gattung *Gephyrocapsa* nach Befunden im Atlantik. *Paläontol. Z.*, **54:** 91-127.

Sato, T., Kameo, K. & Takayama, T. 1991. Coccolith biostratigraphy of the Arabian Sea. *Proc. ODP, Sci. Res.*, **117:** 37-54.

Sato, T. & Takayama, T. 1992. A stratigraphically significant new species of the calcareous nannofossil *Reticulofenestra asanoi*. *In*: K. Ishizaki & T. Saito (Eds). *Centenary of Japanese Micropalentology*. Terra Scientific Pubblishing Company, Tokyo: 457-460.

Shackleton, N.J., Berger, A. & Peltier, W.R. 1990. An alternative astronomical calibration of the lower Pleistocene timescale based on ODP Site 677. *Trans. R. Soc. Edinb. Earth Scien.*, **81:** 251-261.

Sigl, W. & Muller, C. 1975. Identification and correlation of stagnation layers in cores from the eastern Mediterranean. *Rapp. CIESM,* **23:** 277-279.

Sliter, W.V. & Brown, G.R. 1993. Shatsky Rise: seismic stratigraphy and sedimentary record of Pacific paleoceanography since the early Cretaceous. *Proc. ODP, Sci. Res.*, 132: 3-13.

Spaulding, S. 1991. Neogene nannofossil biostratigraphy of Site 723 through 730, Oman Continental Margin, northwestern Arabian Sea. *Proc. ODP, Sci. Res.*, 117: 5-36.

Sprovieri, R. 1993. Pliocene-early Pleistocene astronomically forced planktonic foraminifera abundance fluctuations and chronology of Mediterranean calcareous plankton bioevents. *Riv. It. Paleontol. Strat.*, **99:** 371-414.

Sprovieri, R., Di Stefano, E., Howell, M., Sakamoto, T., Di Stefano, A. & Marino, M. 1998. Integrated calcareous plankton biostratigraphy and cyclostratigraphy at Site 964. *Proc. ODP, Sci. Res.*, **160:** 155-165.

Takayama, T. & Sato, T. 1987. Coccolith biostratigraphy of the North Atlantic Ocean, Deep Sea Drilling Project Leg 94. *IRDSDP,* **94:** 651-702.

Theodoridis, S. 1984. Calcareous nannofossil biozonation of the Miocene and revision of the helicoliths and discoasters. *Utrecht Micropaleontol. Bull.*, **32:** 3-271.

Thierstein, H.R., Geitzenauer, K.R., Molfino, B. & Shackleton, N.J. 1977. Global synchroneity of late Quaternary coccolith datum levels: Validation by oxygen isotopes. *Geology*, **5:** 400-404.

Thunell, R., Williams, D., Tappa, E., Rio, D. & Raffi, I. 1990. Plio-Pleistocene isotope record for ODP Site 653, Tyrrhenian Sea: implication for the paleoenvironmental history of the Mediterranean. *Proc. ODP, Sci. Res.*, **107:** 387-399.

Wallich, G.C. 1877. Observations on coccolithophores. *Ann. Mag. Nat. Hist., Ser.4*, **16:** 322-339.

Wei, W. 1993. Calibration of upper Pliocene-lower Pleistocene nannofossil events with oxygen isotope stratigraphy. *Paleoceanography*, **8:** 85-99.

Young, J. 1998. Neogene. *In*: P. Bown (Ed.). *Calcareous nannofossil biostratigraphy*. British Micropaleontological Society Special Publications Series. Chapman & Hall/Kluwer Academic: 225-265.

Plate 1

XP = cross-polarised light; PL = plain transmitted light. Scale-bar = 5μm

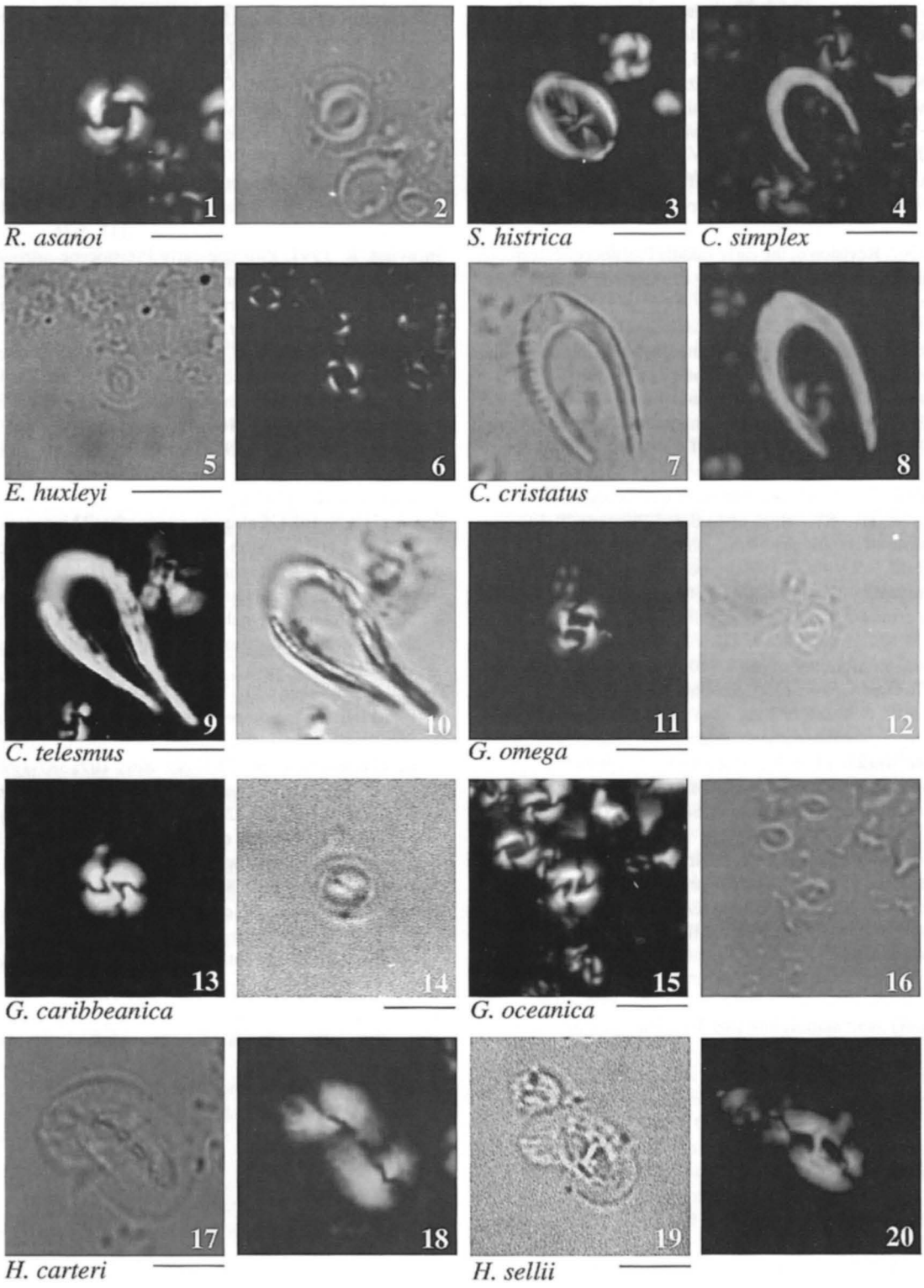

Figs 1, 2: *Reticulofenestra asanoi* Sato & Takayama. DSDP Site 577, 2-4, 43cm; 1, XP, 2, PL. **Fig.3:** *Syracosphaera histrica* Kamptner. DSDP Site 577, 3-3, 44cm, XP. **Fig.4:** *Ceratolithus simplex* Bukry. DSDP Site 577, 1-1, 50cm, XP. **Figs 5, 6:** *Emiliania huxleyi* (Lohmann). DSDP Site 577, 1-1, 50cm; 5, PL, 6, XP. **Figs 7, 8:** *Ceratolithus cristatus* Kamptner. DSDP Site 577, 3-3, 44cm; 7, PL, 8, XP. **Figs 9, 10:** *Ceratolithus telesmus* Norris. DSDP Site 577, 2-6, 40cm; 9, XP, 10, PL. **Figs 11, 12:** *Gephyrocapsa omega* Bukry (>4μm). DSDP Site 577, 2-3, 43cm; 11, XP, 12, PL. **Figs 13, 14:** *Gephyrocapsa caribbeanica* Boudreaux & Hay. DSDP Site 577, 2-6, 103cm; 13, XP, 14, PL. **Figs 15, 16:** *Gephyrocapsa oceanica* Kamptner (>4μm). DSDP Site 577, 3-2, 96cm; 15, XP, 16, PL. **Figs 17, 18:** *Helicosphaera carteri* (Wallich). DSDP Site 577, 2-4, 43cm; 17, PL, 18, XP. **Figs 19, 20:** *Helicosphaera sellii* Bukry & Bramlette. DSDP Site 577, 3-2, 96cm; 19, PL, 20, XP.

Plate 2

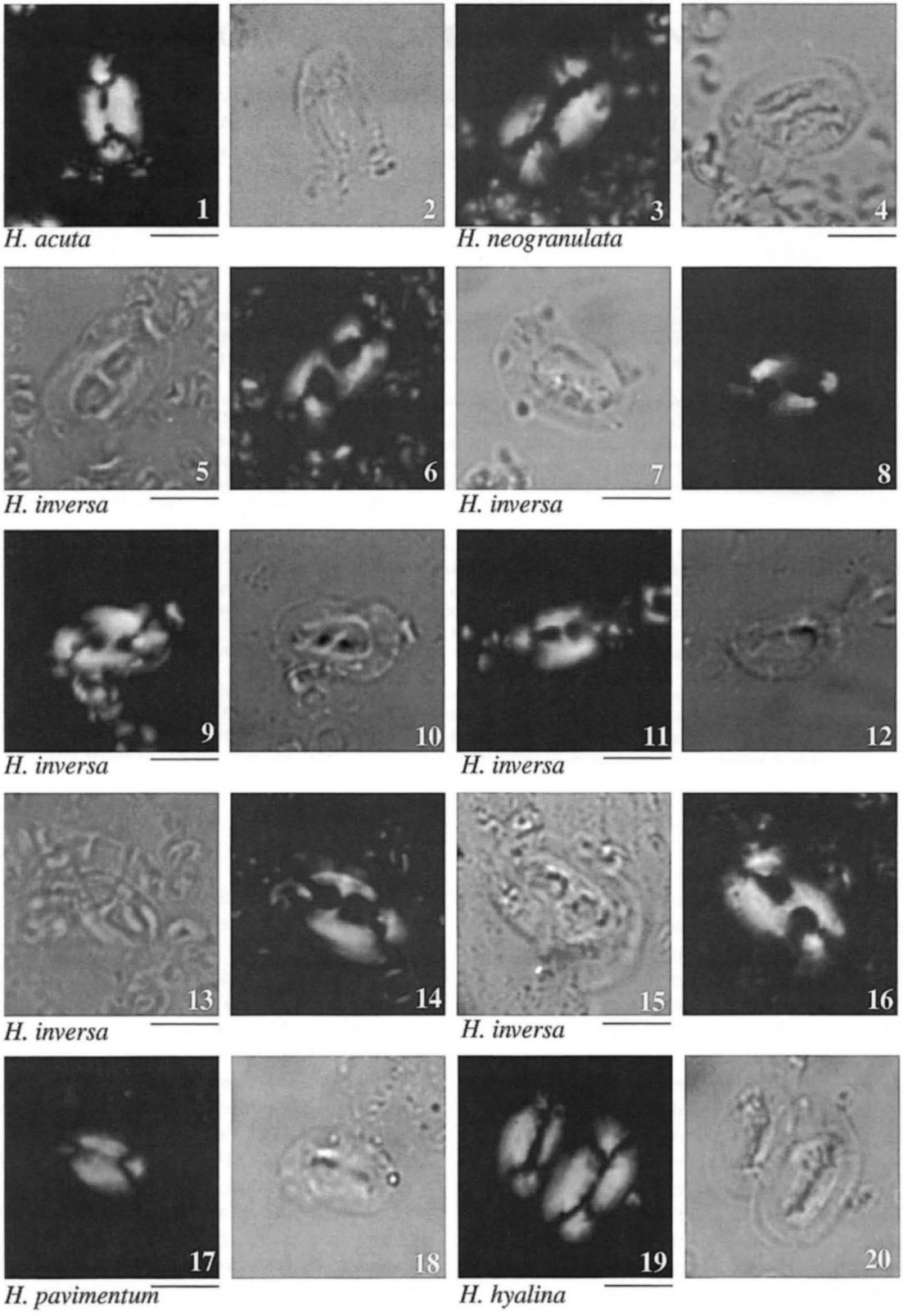

Figs 1, 2: *Helicosphaera acuta* Theodoridis. DSDP Site 577, 2-3, 139cm; 1, XP, 2, PL. **Figs 3, 4:** *Helicosphaera neogranulata* (Gartner). DSDP Site 577, 1-CC, 10-11cm; 3, XP, 4, LP. **Figs 5, 6:** *Helicosphaera inversa* (Gartner). DSDP Site 577, 1-4, 40cm; 5, PL, 6, XP. **Figs 7, 8:** *Helicosphaera inversa* (Gartner). DSDP Site 577, 2-3, 103cm; 7, PL, 8, XP. **Figs 9, 10:** *Helicosphaera inversa* (Gartner). DSDP Site 577, 2-3, 103cm; 9, XP, 10, PL. **Figs 11, 12:** *Helicosphaera inversa* (Gartner). DSDP Site 577, 1-2, 125cm; 11, XP, 12, PL. **Figs 13, 14:** *Helicosphaera inversa* (Gartner). DSDP Site 577, 1-4, 125cm; 13, PL, 14, XP. **Figs 15, 16:** *Helicosphaera inversa* (Gartner). DSDP Site 577, 1-4, 40cm; 15, PL, 16, XP. **Figs 17, 18:** *Helicosphaera pavimentum* Okada & MacIntyre. DSDP Site 577, 1-2, 125cm; 17, PL, 18, XP. **Figs 19, 20:** *Helicosphaera hyalina* (Gaarder). DSDP Site 577, 2-2, 43cm; 19, XP, 20, PL.